

THREE-DIMENSIONAL FLOW STRUCTURE AND TURBULENCE MEASUREMENTS ABOUT A TRAILING EDGE FILM-COOLING BREAKOUT

Yude Chen*

Department of Mechanical Engineering,
Stanford University
488 Escondido Mall Building 500-501R, Stanford, California, 94305, USA
yuchenny@gmail.com

Claude G. Matalanis†

Department of Mechanical Engineering,
Stanford University
488 Escondido Mall Building 500-501R, Stanford, California, 94305, USA
claude.matalanis@gmail.com

John K. Eaton

Department of Mechanical Engineering,
Stanford University
488 Escondido Mall Building 500-501F, Stanford, California, 94305, USA
eatonj@stanford.edu

ABSTRACT

An experimental study is performed to examine the flow structure and turbulence about a model turbine blade trailing edge film-cooling breakout. A model consisting of a NACA 0012 airfoil modified to have a realistic trailing edge breakout was placed in a water tunnel. The breakout geometry is based on approximate measurements of several modern turbine blades. Reynolds number based on chord length is approximately 56,000. High resolution particle image velocimetry is performed to examine the flow field and turbulence about the breakout region. The results suggest that the geometry and cooling flow result in a highly three-dimensional flow in the immediate vicinity of the breakout. Also, the cooling flow significantly increases the turbulent kinetic energy immediately downstream of the breakout. All of this implies strong mixing between the mainstream flow and cooling flow that is likely responsible for degrading film-cooling effectiveness at the trailing edge.

INTRODUCTION

The blades in the high pressure turbines of jet engines are subjected to high temperature flow at high velocity. Such conditions can decrease the life of these components dramatically if they are not cooled properly. Thus, high pressure turbine blades are often cooled by passing lower temperature compressor air through internal cooling passages and out through film cooling holes along the blade surface. The trailing edge, however, is typically too thin to accommodate internal cooling passages. A trailing edge breakout, as shown in figure 1, is often used to cool the trailing edge. In a typical breakout, approximately the last 5% of the blade on the pressure side are cut away along the span creating slots

separated by tapered lands. The cooling flow exits through these rectangular slots in the streamwise direction in order to cool the trailing edge. Since each land is positioned directly between two substantial cooling slots, it is intuitive that the trailing edge should be well cooled compared to the rest of the blade. In practice, however, the opposite has often been observed, and the trailing edge has been found to deteriorate faster than the rest of the blade.

The main parameter used to quantify the amount of cooling achieved locally on the blade is the film cooling effectiveness, η , defined as

$$\eta = \frac{T_\infty - T_{aw}}{T_\infty - T_c}, \quad (1)$$

where T_∞ is the hot mainstream temperature, T_{aw} is the adiabatic wall temperature at the blade surface, and T_c is the temperature of the cooling flow. Values of η near zero imply poor effectiveness, while values of η near unity imply excellent effectiveness. Clearly, higher values of η are desirable in order to minimize blade deterioration and maximize life.

Film cooling at the trailing edge has been researched heavily both experimentally and computationally over the past 50 years. Previous experiments have indicated that η is strongly dependent upon the blowing ratio, which is the mass flux of the coolant divided by the mass flux of the mainstream. In addition, other parameters have been found to be important. Papell (1960), Sivasegaram and Whitelaw (1969), and Mehlman (1990) examined the influence of the slot angle upon film cooling effectiveness and found that in general, η increases as the slot angle is made more tangential to the mainstream flow. The work of Samuel and Joubert (1965) and Metzger et al. (1968) indicated similar trends. Kacker and Whitelaw (1968, 1969) and Taslim et al. (1992) examined the effect of varying the ratio of slot lip thickness to jet opening and found that increasing this ratio tended to decrease η . Rastogi and Whitelaw (1972a) studied slots similar to the ones found in gas-turbine combustors and found

*Currently Hardware Engineer, Sun Microsystems, 12 Network Circle, Menlo Park, California 94025

†Currently Research Engineer, United Technologies Research Center, 411 Silver Lane, East Hartford, Connecticut 06108

the results similar to 2D results. Kim et al. (2005) found that the acceleration of the mainstream flow had a significant effect on film cooling effectiveness. Also, Cunha and Chyu (2006) found that details in the geometry such as cut-back length of the breakout were important. Finally, the work of Martini et al. (2005) showed that in addition to the outside geometry of the blade, the inner geometry of the cooling flow passage feeding the breakout was also important.

Numerical techniques for predicting film cooling effectiveness have also been researched extensively. Many of the trends discussed above have also been shown computationally. Nicoll and Whitelaw (1966), Pai and Whitelaw (1971), and Rastogi and Whitelaw (1972b) have developed general methods for determining η and the heat transfer coefficient. Paxson and Mayle (1989) successfully predicted the effect of the mainstream thermal boundary layer upon η .

Most of the experiments and computations discussed above pertain to two-dimensional slot geometries. Holloway et al. (2002a,b) performed steady and unsteady RANS on a three-dimensional geometry similar to the one shown in figure 1. They found that their results tended to overpredict η when compared to experimental results and suggested that this could be due to coherent unsteadiness in the cooling flow of the experiments. Medic and Durbin (2005) later performed unsteady RANS with and without a coherent oscillation of the coolant flow. The results showed that the oscillation resulted in shedding of spanwise vorticity at the interface between the coolant and the mainstream which led to increased mixing and significantly lower film cooling effectiveness. They also showed that the spanwise vortices would later form vortex loops, further enhancing mixing. With the periodic oscillation imposed, the computed η better matched what had been seen in experiments.

The work of Medic and Durbin suggests a possible mechanism for the mixing of cooling flow with mainstream flow, however, the periodic oscillation imposed was rather arbitrary, thus, it is unknown whether or not the mechanism shown is in fact the cause of reduced film cooling effectiveness at the trailing edge breakout. There have been no spatially resolved turbulence measurements of the flow in the near field of a realistic trailing edge breakout geometry. Uzol and Camci (2001a,b) made such measurements to determine aerodynamic losses due to film cooling, however, only the distribution of mean flow magnitude in one plane was shown, thus, the three-dimensional structure and turbulence characteristics remain unknown.

The goal of this work is to present highly resolved flow measurements about a model turbine blade trailing edge breakout. We use a realistic three-dimensional breakout geometry and perform two-dimensional PIV measurements of the flow about the breakout in three planes along the span. The data reveal key aspects of the three-dimensional flow structure and turbulence. These measurements also allow for detailed comparison to computational models.

EXPERIMENTAL APPARATUS

Water tunnel measurements on a model turbine blade with a trailing edge breakout are conducted. A symmetric airfoil is chosen to avoid measurement difficulties associated with highly curved flows, but to maintain a favorable pressure gradient along the airfoil, the tunnel walls at the airfoil are modified with inserts to create a two-dimensional contraction. The details of the breakout geometry were designed using approximate measurements of several modern turbine blades. Complete airfoil and contraction geometry is avail-

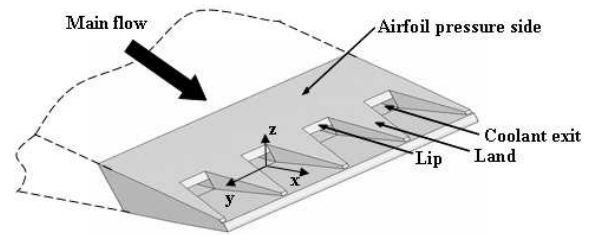


Figure 1: The trailing edge breakout geometry.

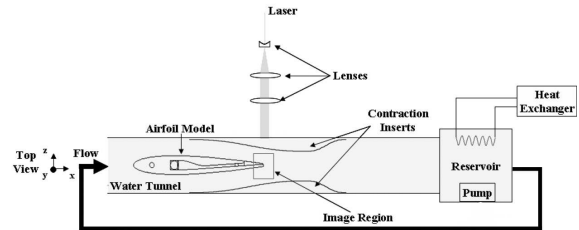


Figure 2: Top view of the entire experimental apparatus.

able from the authors.

Water tunnel

A schematic of the entire experimental apparatus is shown in figure 2. The turbine blade model and contraction inserts are placed in a recirculating water tunnel with a 51 mm \times 102 mm test section and a maximum freestream velocity of 0.38 m/s. Flow through the tunnel is driven using a 0.37 kW centrifugal pump, and the water temperature is held constant at 22°C using a heat exchanger in the tunnel reservoir.

The contraction inserts are designed using CFD and placed on the wall of the tunnel above and below the airfoil. The contraction begins approximately 43 mm upstream of the airfoil leading edge and reduces the tunnel area gradually to a minimum of one-half the nominal area at a point 42 mm downstream of the trailing edge. The inserts then taper off and end roughly 220 mm downstream of the trailing edge.

Airfoil model

The model used in these experiments consists of a NACA 0012 airfoil modified to include a trailing edge breakout. It was fabricated in Waterclear resin using stereolithography. The base airfoil has a chord length of 150 mm and a span of 49 mm. Rubber gaskets are used to prevent flow between the tips of the airfoil and the tunnel walls. All tests are conducted at a Reynolds number based on chord length of approximately 56,000. The airfoil is set at a zero angle of attack.

We modify the airfoil to include a trailing edge breakout as follows. The last 5.7% of the base airfoil are discarded to create a blunt trailing edge. Thus, the actual chord length of the airfoil, c , is 141.5 mm. On the pressure side of the airfoil, the final 21 mm comprises the actual breakout region shown in figure 1. Four rectangular cooling holes, each 5 mm \times 2.5 mm are oriented in the streamwise direction. They are separated by trapezoidal lands, each of which extends down to 0.87 mm upstream of the trailing edge. The lip above each cooling hole is 1.9 mm thick.

To supply the cooling holes, an inlet hole oriented in the spanwise direction is placed at the quarter-chord point. Cooling flow enters there into a manifold designed to smoothly accelerate and distribute the flow to each cooling hole. The supply is fed by an auxiliary pump placed in the tunnel reservoir, and the overall flow rate is controlled by a Dwyer 2 GPM rotameter-type flowmeter with a built in valve.

PIV system

The PIV system used is a commercial system from TSI, Inc. The laser used for illumination is a New Wave dual head pulsed Nd:YAG laser capable of 50 mJ/pulse. The CCD camera is a 12 bit 1.3 megapixel TSI PIVCAM 13-8. Images are acquired with 300 μ s spacing between images of a pair and sent through a framegrabber to a Dell Precision workstation. Timing of the laser, camera, and framegrabber are achieved with the TSI Insight software and synchronizer (Model 610034).

Flow measurements about the trailing edge breakout region are made using two-dimensional PIV. We use three lens elements (two spherical and one cylindrical) to create a sheet oriented in the XZ plane which is approximately 0.5 mm thick and 20.6 mm wide. The sheet passes directly through the transparent inserts and airfoil allowing measurements both above and below the airfoil without realigning the laser optics. The tunnel wall at the region of interest is fitted with a glass insert to allow proper imaging of the flow by the CCD camera. A square calibration grid with 1 mm spacing placed in the region of interest is used to relate pixel displacement to physical distance. The magnification factor is approximately 0.02 mm/pixel.

All PIV processing is performed using PIVLab, a software package written in Matlab and developed at Stanford University (Han 2001). This software uses iterative image-shift cross-correlation PIV and Gaussian fitting for subpixel resolution. The smallest interrogation region is 32×32 pixels, and all images are processed using 50% overlap. Thus, the spatial distance between neighboring data points is approximately 0.3 mm. For each data set, 1000 image pairs are acquired.

Uncertainty

For the PIV data, the uncertainty is calculated taking into account a subpixel estimator uncertainty of ± 0.2 pixels (Han 2001), laser sheet alignment uncertainty of $\pm 1^\circ$, and a statistical uncertainty of ± 0.028 m/s in the turbulent region and ± 0.0034 m/s outside the turbulent region. Other sources of uncertainty including timing, particle lag, seeding uniformity, and calibration grid accuracy are minor. The total uncertainty with 95% confidence intervals is ± 0.048 m/s in the turbulent region and ± 0.039 m/s outside the turbulent region.

The uncertainty in cooling flow rate based on the published accuracy and resolution of the rotameter is ± 0.074 GPM.

RESULTS

The coordinate system used to present this work is illustrated in figure 3. To nondimensionalize the spanwise coordinate, we use d , the spanwise distance from the center of a breakout hole to the center of the neighboring land. Measurements of the flow at the trailing edge breakout are conducted in the XZ plane at three spanwise stations: the

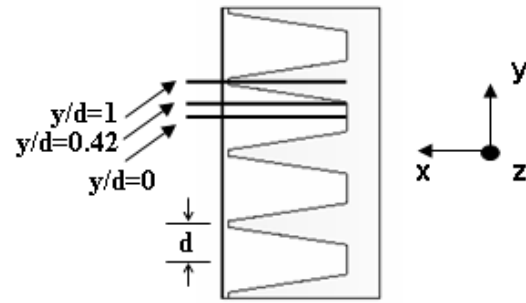


Figure 3: Locations of the three PIV measurement planes. breakout ($y/d = 0.0$), the land ($y/d = 1.0$), and the intersection ($y/d = 0.42$).

The amount of cooling flow used is quantified by the blowing ratio, M , where

$$M = \frac{(\rho u)_{coolant}}{(\rho u)_{mainstream}}. \quad (2)$$

Here, the coolant and mainstream fluid are both water, thus,

$$\rho_{coolant} = \rho_{mainstream}. \quad (3)$$

The velocity used for nondimensionalizing all flow data is the reference velocity, $u_{ref} = 0.87$ m/s, which is the freestream velocity measured 10 mm downstream of the trailing edge. Finally, the coolant velocity, $u_{coolant}$, is calculated from the volume flow rate of coolant measured at the rotameter valve, i.e.,

$$u_{coolant} = \frac{\dot{Q}_{coolant}}{A_{coolant}}, \quad (4)$$

where $\dot{Q}_{coolant}$ is the volume flow rate of coolant to the entire breakout, and $A_{coolant}$ is the total area that coolant may exit from. Thus,

$$M = \frac{u_{coolant}}{u_{ref}}. \quad (5)$$

At each station, three blowing ratios are examined: 0.0, 1.0, and 1.5. The uncertainty in blowing ratio based on the rotameter uncertainty, the uncertainty in u_{ref} , and the uncertainty in the breakout geometry is ± 0.13 .

We begin by examining the mean flow field of the vertical velocity component only. Figure 4 shows contours of w/u_{ref} at each spanwise position for the nominal case of no cooling flow ($M = 0$). The geometry of the breakout region is also drawn to show the position and orientation of the airfoil and breakout. In all figures, the breakout is on the upper side of the airfoil. Due to reflections from the surface of the blade, it is not possible to collect data closer than 1 mm to the surface, thus, all data points closer than that have been removed. Above and below the airfoil, the flow closely follows the surface of the geometry with slightly negative w values on the upper side and slightly positive values on the lower side. The flow field at all three positions is fairly similar, however, at the land ($y/d = 1.0$), we see a small region of vertical velocity deficit immediately behind the airfoil and just above the chord line, but this difference is quite small. Thus, for $M = 0$, the flow about the breakout is fairly uniform in the spanwise direction implying that the three-dimensional geometry causes the flow field to be only weakly three-dimensional.

Next, we examine the effects of adding cooling flow. Note that we expect the cooling flow to produce strong advection

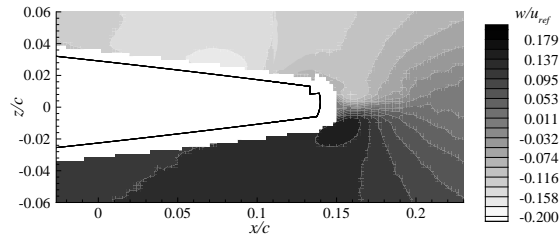
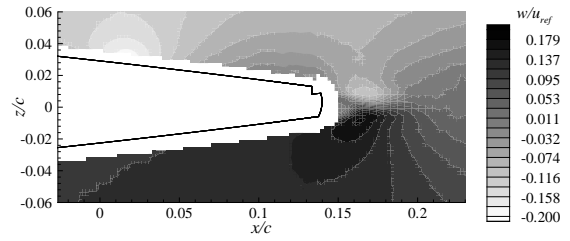
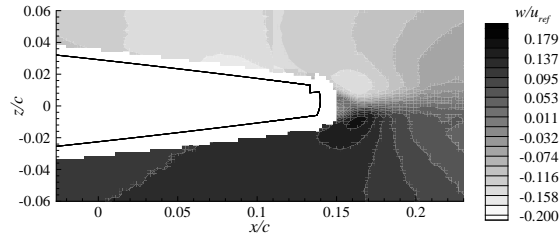
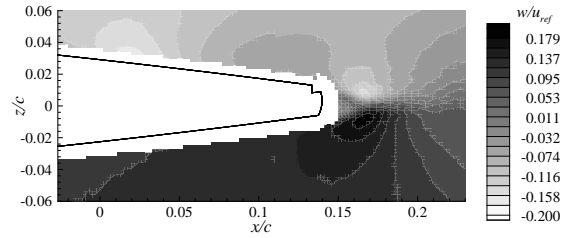
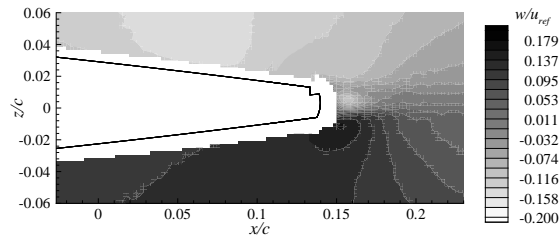
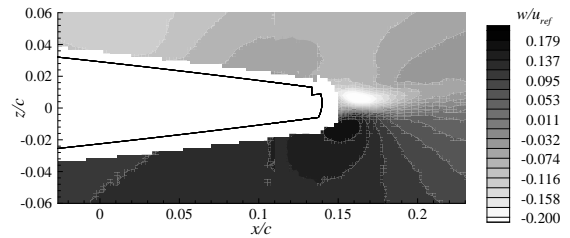
(a) $y/d = 0.0$ (a) $y/d = 0.0$ (b) $y/d = 0.42$ (b) $y/d = 0.42$ (c) $y/d = 1.0$ (c) $y/d = 1.0$

Figure 4: Contours of lift direction velocity (w -field) with no cooling flow ($M = 0.0$).

in the x -direction immediately downstream of the coolant exits ($y/d = 0.0$). The measured velocity magnitude field indicated that this is indeed the case, however, by examining only the vertical velocity component and not including the streamwise component, we neglect this strong advection. This allows us to examine more subtle aspects of the flow field caused by the cooling flow. Figure 5 shows contours of the same locations as the previous figure now with $M = 1.0$. The flow at the breakout and intersection (figure 5a, b) is quite similar to the $M = 0$ case, but the flow at the land displays a strong downwash immediately downstream of the trailing edge. Thus, with a blowing ratio of 1.0, the flow field is much more three-dimensional.

For the $M = 1.5$ case (figure 6), we see the same effect to a greater extent. Again, a strong downwash occurs immediately downstream of the trailing edge at the land.

To examine this more quantitatively, in figure 7, we consider w -velocity profiles with respect to the z -direction at $x/c = 0.16$. Here, we clearly see the increase in downwash that occurs as we move from the breakout to the land. For this case with $M = 1.5$, the maximum difference in w is approximately $20\%u_{ref}$. This indicates the existence of significant streamwise vorticity which is likely due to the three-dimensional geometry of the breakout and the cooling flow. Thus, as flow exits from the breakout at $y/d = 0.0$, it turns about the edge of the land then heads downward producing the apparent downwash at $y/d = 1.0$. While we can only observe this downwash at the trailing edge, it is likely that the streamwise vortices originate farther up-

Figure 5: Contours of lift direction velocity (w -field) for a blowing ratio, $M = 1.0$.

stream along the sides of the land. This could lead to mixing of the mean flow with the cooling flow, and bring more of the hot mainstream flow into contact with the blade surface.

The cooling flow also has an effect on the turbulence about the breakout. In figure 8, we examine the effects upon the turbulent kinetic energy field. Since the spanwise velocity component is not available from 2D PIV, we define k as

$$k \approx \frac{3}{4} (u'u' + w'w'). \quad (6)$$

Clearly, the turbulent kinetic energy immediately downstream of the trailing edge at the breakout ($y/d = 0.0$) is increased significantly due to the cooling flow. Peak values of k are approximately doubled. Note also that in figure 8b, the cooling flow has caused the wake to move upwards slightly. This is consistent with the streamwise vorticity indicated in the mean flow contours: the flow is turned downwards at the land ($y/d = 1.0$), and upwards at the breakout ($y/d = 0.0$).

CONCLUSIONS

High resolution PIV measurements of the flow about a realistic trailing edge breakout were performed providing detailed information about the mean flow field and turbulence statistics about the breakout region. Important features of the three-dimensional flow structure were revealed.

An examination of the vertical velocity component field has indicated the existence of streamwise vorticity that is

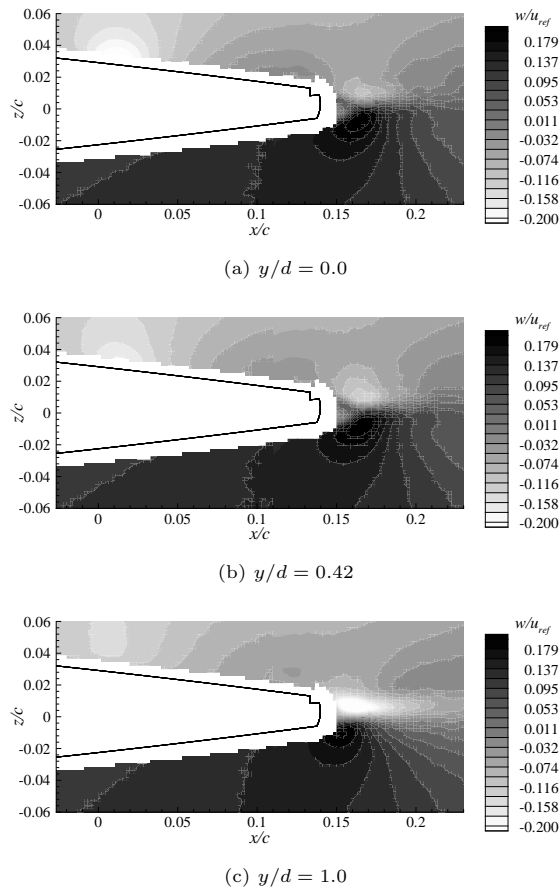


Figure 6: Contours of lift direction velocity (w -field) for a blowing ratio, $M = 1.5$.

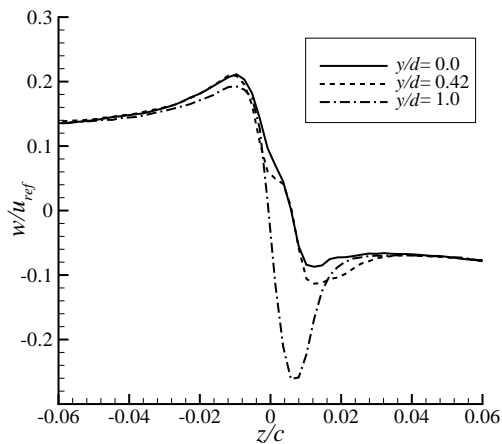
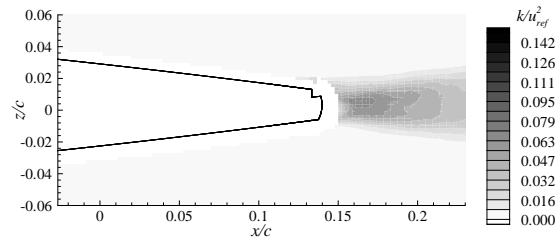
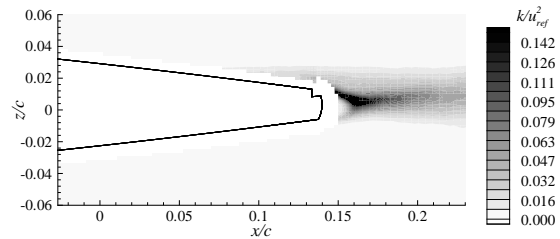


Figure 7: Vertical profiles of the w velocity component at $x/c = 0.16$ at the three spanwise positions for $M = 1.5$.



(a) $M = 0.0, y/d = 0.0$



(b) $M = 1.5, y/d = 0.0$

Figure 8: Contours of turbulent kinetic energy at the breakout ($y/d = 0.0$) for two blowing ratios.

shed between the breakout and the lands causing strong downwash behind the lands. This vorticity may also be partially responsible for lowering film cooling effectiveness at the trailing edge by bringing more of the mainstream flow into contact with the blade surface.

The turbulent kinetic energy field indicates a large increase in turbulent fluctuations immediately behind the blade due to the cooling flow. Movement in the wake visible in the turbulent kinetic energy field also implies the existence of streamwise vorticity as mentioned above.

Finally, although measurements directly on the blade surface and inside the breakout were not possible, the measurements made do allow for direct comparison to computational models. Thus, the performance of models inside the breakout can be inferred from their performance at the regions measured.

ACKNOWLEDGEMENTS

The authors would like to acknowledge Mr. Jong-Wook Joo for his assistance with the detailed design of the blade geometry, and Mr. Frank Medina of the University of Texas, El Paso for fabricating the airfoil model. Financial support was received from the Air Force Office of Scientific Research and the General Electric University Strategic Alliance. Mr. Chen was supported by a National Science Foundation Graduate Fellowship.

REFERENCES

- Cunha, F. J., and Chyu, M. K., 2006, "Trailing-edge cooling for gas turbines", *Journal of Propulsion and Power*, Vol. 22, pp. 286-300.
- Holloway, D. S., Leylek, J. H., and Buck, F. A., 2002a, "Pressure-side bleed film cooling: part 1, steady framework for experimental and computational results", ASME Turbo Expo 2002, GT2002-30471.
- Holloway, D. S., Leylek, J. H., and Buck, F. A., 2002b, "Pressure-side bleed film cooling: part 2, unsteady framework for experimental and computational results", ASME

Turbo Expo 2002, GT2002-30472.

Kacker, S. C., and Whitelaw, J. H., 1968, "The effect of slot height and slot turbulence intensity on the effectiveness of the uniform density, two-dimensional wall jet", *ASME Journal of Heat Transfer*, Vol. 90, pp. 469-475.

Kacker, S. C., and Whitelaw, J. H., 1969, "An experimental investigation of the influence of slot lip thickness on the impervious-wall effectiveness of the uniform-density, two dimensional wall jet", *International Journal of Heat and Mass Transfer*, Vol. 12, pp. 1196-1201.

Kim, Y. W., Coon C., and Moon, H. K., 2005, "Film-cooling characteristics of pressure-side discharge slots in an accelerating mainstream flow", ASME Turbo Expo 2005, GT2005-69061.

Martini, P., Schulz, A., and Bauer, H. J., 2005, "Film cooling effectiveness and heat transfer on the trailing edge cutback of gas turbine airfoils with various internal cooling designs", ASME Turbo Expo 2005, GT2005-68083.

Medic, G., and Durbin, P. A., 2005, "Unsteady effects on trailing edge cooling", *ASME J. Fluids Engineering*, Vol. 127, pp. 388-392.

Mehlman, B. P., 1990, "Experimental slot film cooling effectiveness measurements for varying injection angles in accelerating and non-accelerating flows", M.S. thesis, Massachusetts Institute of Technology, Boston, MA.

Metzger, D. E., Carper, H. J., and Swank, L. R., 1968, "Heat transfer with film cooling near nontangential injection slots", *Journal of Engineering for Power*, pp. 157-163.

Nicoll, W. B., and Whitelaw, J. H., 1966, "The effectiveness of the uniform density, two dimensional wall jet", *International Journal of Heat and Mass Transfer*, Vol. 10, pp. 623-639.

Pai, B. R., and Whitelaw, J. H., 1970, "The prediction of wall temperature in the presence of film cooling", *International Journal of Heat and Mass Transfer*, Vol. 14, pp. 409-426.

Papell, SS, 1960, "Effect on gaseous film cooling injection through angled slots and normal holes", NASA TN-D-299.

Paxson, D. E., and Mayle, R. E., 1989, "The influence of a mainstream thermal boundary layer on film effectiveness", *Journal of Turbomachinery*, Vol. 111, pp. 491-496.

Rastogi, A. K., and Whitelaw, J. H., 1972a, "The effectiveness of three-dimensional film-cooling slots - I. Measurements", *International Journal of Heat and Mass Transfer*, Vol. 16, pp. 1665-1672.

Rastogi, A. K., and Whitelaw, J. H., 1972b, "The effectiveness of three-dimensional film-cooling slots - II. Predictions", *International Journal of Heat and Mass Transfer*, Vol. 16, pp. 1673-1681.

Samuel, A. E., and Joubert, P. N., 1965, "Film cooling of an adiabatic flat plate in zero pressure gradient in the presence of a hot mainstream and cold tangential secondary injection", *ASME Journal of Heat Transfer*, Vol. 87, pp. 409-418.

Sivasegaram, S., and Whitelaw, J. H., 1969, "Film cooling slots: the importance of lip thickness and injection angle", *Journal of Mechanical Engineering Science*, Vol. 11, pp. 22-27.

Taslim, M. E., Spring, S. D., and Mehlman, B. P., 1992, "Experimental investigation of film cooling effectiveness for slots of various exit geometries", *Journal of Thermophysics and Heat Transfer*, Vol. 6, pp. 302-307.

Uzol O., and Camci, C., 2001a, "Aerodynamic loss characteristics of a turbine blade with trailing edge coolant ejection: part 1 - effect of cutback length, spanwise rib spacing, free-stream Reynolds number, and chordwise rib length

on discharge coefficients", *Journal of Turbomachinery*, Vol. 123, pp. 238-248.

Uzol O., and Camci, C., 2001b, "Aerodynamic loss characteristics of a turbine blade with trailing edge coolant ejection: part 2 - external aerodynamics, total pressure losses, and predictions", *Journal of Turbomachinery*, Vol. 123, pp. 249-257.